

Investigating the Synergistic Effect of *Chamaecostus cuspidatus* Leaf Extract and para-Coumaric Acid on Streptozotocin-induced Diabetic Nephropathy in Wistar Rats

Menaka Priya Balaji and Devi Rajeswari V.*

Department of Bio-Medical Science, School of Bioscience and Technology, Vellore Institute of Technology, Vellore, 632014, INDIA

*vdevirajeswari@vit.ac.in

Abstract

The research investigation aims to examine the impairment of endothelial function in a Wistar rat model of insulin-resistant diabetes mellitus triggered by a high-fat diet and administration of 40mg/kg streptozotocin. *Chamaecostus cuspidatus* leaf extract, para-coumaric acid and a combination of para-coumaric acid and *Chamaecostus cuspidatus* leaf extract were administered to diabetic animals. A standard control group was administered 100mg/kg of metformin. Interestingly, the findings of this investigation indicated that *Chamaecostus cuspidatus* extract treatment effectively regulated glucose levels ($P < 0.05$), while para-coumaric acid reduced lipoprotein levels ($P < 0.0001$), the combination showed effectively regulated hematological parameters and increased the antioxidant efficacy ($P < 0.0001$).

Moreover, this combined treatment has also been observed to enhance antioxidant enzymes of SOD, CAT, GSH and GPX activities and also prevent lipid peroxidation and ROS levels in the kidney tissue. The histopathology results of the kidney renal cells revealed that the administration of synergistic treatment led to a decrease in inflammation of a lower grade as well as a recovered endothelium layer. The experiment revealed that the synergy between *Chamaecostus cuspidatus* and para-coumaric acid regulates biochemical characteristics and enhances antioxidants, thus suggesting an effective treatment for diabetic nephropathy.

Keywords: Antioxidant, Diabetic glomerulosclerosis, para-Coumaric acid, Insulin plant, Oxidative stress marker.

Introduction

Diabetes mellitus is a global pandemic, with roughly 537 million persons aged 21–79 affected, as reported by the International Diabetes Federation (IDF). The number is expected to rise to 783 million by 2045^{6,21}. Diabetes mellitus increases the likelihood of developing atherosclerosis 2–3-fold, leading to persistent macrovascular and microvascular diseases. Obesity and insulin resistance play significant roles in the lipolysis pathway, ultimately leading to liver lipotoxicity and affecting bloodstream lipid parameters. In

addition, these conditions can have a detrimental effect on kidney function which increases the microlevel of albumin in the urine and eventually leads to diabetic glomerulosclerosis²³.

Reducing the incidence of diabetic nephropathy complications is a major clinical concern due to the increasing prevalence of type 2 diabetes which may lead to metabolic disorders and may disrupt the endothelium layer in the kidney. Pathological stress activates antioxidant enzymes such as superoxide dismutase (SOD), catalase (CAT), glutathione peroxidase and non-enzymatic antioxidant of reduced glutathione via the protein kinase RNA-like endoplasmic reticulum kinase (PERK) and Nuclear Factor Erythroid 2-Related Factor 2 (Nrf2) pathway⁵. Metabolic reactive oxygen species (ROS) and an imbalance in nitric oxide (NO) bioavailability in the endothelium led to the dissociation of nitric oxide synthase and impaired the electron transport chain (ETC), resulting in endothelial injury in the kidney. If the endothelium layer continuously generates superoxide, it can be transformed into a highly reactive oxidant of peroxynitrite^{4,7}.

Reduced antioxidant and elevated oxidative stress cause deterioration of the endothelium layer, culminate in hyperfiltration, proteinuria and the progression of glomerulosclerosis. Chronic hyperglycemia, dyslipidemia and oxidative stress are important conditions not fully addressed by existing medications and should be the primary focus of treatment.

Synergistic approaches have demonstrated the potential to mitigate the drawbacks of side effects and to enhance the efficacy of treatments by leveraging multiple mechanisms of action. While synthetic medication can have targeted effects, they may also exhibit unwanted side effects. In contrast, herbal medications often demonstrate a broader range of benefits including antioxidant and pharmacological properties, which can help in restore and to balance the body's natural functions¹⁹. *Chamaecostus cuspidatus* is frequently recognized as the insulin plant and is also referred to as *Costus igneus* and spiral flag. The insulin plant leaf exhibits various benefits including effects that might assist with managing diabetes, combat oxidative stress, reduce inflammation and inhibit microbial growth. These effects are linked to the presence of specific compounds including insulin-like protein, quercetin⁹, diosgenin¹⁰ and β -amyrin^{11,16}.

The potential of traditional plant leaves and natural polyphenols, particularly hydroxyl compound of hydroxycinnamic acid (*para*-coumaric acid), to mitigate oxidative stress and reduce the risk of chronic disease including heart disease, cancer and neurodegenerative disorders are substantial. This study hypothesizes that combination therapy of *C. cuspidatus* leaf extract with *para*-coumaric acid can effectively regulate diabetes and reduce microvascular complications. Therefore, this research investigates the synergistic effects of combination therapy involving *C. cuspidatus* and *para*-coumaric acid on biochemical markers, antioxidant and oxidative stress parameters and the histological integrity of renal tissues in streptozotocin-triggered diabetic Wistar rats.

Material and Methods

Chemicals: Streptozotocin and *para*-coumaric acid were purchased from Sigma Aldrich. All remaining antioxidant compounds were purchased from the appropriate vendor at commercial outlets.

Authentication of plant sample: Prof. P. Jayaraman, Director of Plant Anatomy Research Centre (PARC) at West Tambaram, Chennai, taxonomically recognized *C. cuspidatus*. The identification was carried out using the permission number: PARC/2022/4736.

***Chamaecostus cuspidatus* leaf extract preparation:** The *C. cuspidatus* plant leaves were picked, cleaned and dried in the shade. The leaf sample was powdered using a laboratory milling machine and then filtered using a 0.25-mm screen. Following this, 10 grams of *C. cuspidatus* leaf powder was soaked in 100 mL of methanol and placed in a shaking incubator for 48–72 hours (maceration). The extract was strained through muslin fabric and concentrated using a rotary evaporator. The methanol crude of *C. cuspidatus* was concentrated using a rotary evaporator and subsequently freeze-dried. The resulting powder was administered to animals as a 5% DMSO solution.

In-vivo experiments

Ethical consideration: All operations on animals were conducted with the authorization of the institutional animal ethics committee (IAEC; Ethical identification number: VIT/IAEC/22/Dec 22/14). The animals were housed at 27°C, 45%–65% controlled humidity levels and a 12-hour day-night cycle, with unrestricted access to nourishment and hydration³.

Induction of obesity and diabetes: Thirty-six healthy male *Rattus norvegicus* rats, aged 5–6 weeks and weighing 150–170 g, were chosen and were fed standard and high-fat diets for the first 15 days²². After 2 weeks, animals weighing 250–300 g were fasted overnight and induced with diabetes by intraperitoneal injection of a low dose of streptozotocin (40 mg/kg STZ) dissolved in 0.1M sodium citrate buffer (pH 4.5)¹². Rats were observed for 3–4 days, then they were fasted for 12 hours to evaluate their blood glucose level.

Glucose levels were measured with the Accu-Check quick glucometer and test strips. As a result, the rats significantly showed a blood glucose level of 250 mg/dL which exceeded the normal range.

Experimental design: There were six groups of rats with six rats in each group in this investigation.

Control (G-1): The animals were given a standard diet and were orally given a solution containing 5% DMSO.

STZ and obesity (G-2): Diabetes was induced in the rats using 40mg/kg of streptozotocin and given a high-fat diet for the first 15 days.

Metformin (G-3): A high-fat diet with streptozotocin-diabetic rats in this group administered 100mg/kg/day of metformin¹.

***C. cuspidatus* 100mg/kg (G-4):** A high-fat diet with streptozotocin-diabetic rats administered 100mg/kg/day of *C. cuspidatus* extract⁸.

***para*-Coumaric acid 100mg/kg (G-5):** High-fat diet with streptozotocin-diabetic rats received 100mg/kg/day of *para*-Coumaric acid².

Synergistic treatment (G-6): High-fat diet with streptozotocin-diabetic rats received *C. cuspidatus* 100mg/kg/day and *para*-Coumaric acid 20mg/kg/day. Rats were euthanized after the therapy, blood was obtained by cardiac puncture and the kidney was dissected and rinsed with cold phosphate-buffered saline (PBS). Kidney samples were homogenized and prepared for microsomes for biochemical and antioxidant assays. The remaining samples were preserved in 10% formalin for histopathological investigation.

Biochemical parameters estimation: At the end of the research period, the animals were fasted overnight and then sacrificed. Blood was collected by heart puncture and put into EDTA tubes (0.5 mL). The serum was separated by centrifugation at 2500 rpm for 15 minutes and kept at -80°C for future use. HbA1c levels in fasting serum were determined using the HPLC technique. Serum lipid parameters were assessed using a commercial kit approach. Serum total protein was determined using the biuret technique. The blood urea nitrogen (BUN) in the kidney marker was evaluated using the kinetic UV test technique. Serum creatinine and uric acid levels were measured using the creatinine enzymatic technique and the uricase/peroxidase methods.

Antioxidant and oxidative stress evaluation: Kidney tissue samples were homogenized in 0.25M sucrose solution and centrifuged. The resulting supernatant was stored at -72°C. Protein concentration was quantified using the Bradford method¹⁵. Homogenate samples were analyzed for

antioxidant parameters including superoxide dismutase (SOD)¹³, catalase (CAT)¹⁸, reduced glutathione (GSH)¹⁴, glutathione peroxidase (GPX)¹⁷ as well as lipid peroxidation [malondialdehyde (MDA)]²⁰. Additionally, oxidative stress indicator nitric oxide and reactive oxygen species (ROS)¹⁴ were assessed.

Histopathological examination: The kidney tissue slice was examined and evaluated using the Hematoxylin and Eosin (H&E) staining method. The pathologist inspected the tissues. The histological examination of the kidney classes is shown in table 1.

Table 1
Categorization of histological features in the endothelial layer of the kidney.

Class of severity	Kidney
Healthy	Normal structures and arrangement
Grade I	Glomerular basement membrane thickening
Grade II	Mesangial expansion/dilation
Grade III	Kimmelstiel Wilson lesion
Grade IV	Diffuse and nodular glomerulosclerosis

Statistical analysis for *in vivo* research: The analysis of statistical results was performed employing Graph Pad Prism (version 8.0.2) with data provided as mean \pm standard error mean. Significance was set at $p < 0.05$. Statistical comparisons were conducted using One-way ANOVA with Tukey's post hoc test for biochemical, antioxidant analysis and oxidative stress investigation and two-way ANOVA with the least significant difference test for body weight.

Results and Discussion

Oral glucose tolerance test (OGTT), HbA1c and body weight - Fig. 1a: OGTT shows the variations in fasting oral glucose tolerance test (OGTT) results across all groups ($P < 0.05$). Glucose administration significantly elevated sugar

sensitivity levels at 0, 30, 60 and 120 minutes. Groups 2,3,4,5 and 6 showed the pre-diabetes condition after 15 days of a high-fat diet. Following streptozotocin-induced diabetes on day 22, all groups except the normal control displayed hyperglycemia. During the treatment period, the metformin-treated group (3) demonstrated a gradual increase in blood glucose levels over three weeks. In contrast, groups 4 and 5 exhibited a gradual decrease, while the synergistic group (6) showed a significant reduction in blood glucose levels.

The bar graph of HbA1c levels bar graph (glycated hemoglobin) in fig. 1b was comparable across all groups ($P < 0.05$). After 21 days of treatment, groups 3, 4 and 6 exhibited a significant reduction in 120-minute glucose concentration compared to group 5. Group 5 demonstrated slightly higher glucose levels than the other treatment groups, suggesting that para-coumaric acid may have a limited effect on glucose regulation. The finding from group 6 indicates the synergistic therapy of *C. cuspidatus* and para-coumaric acid significantly decreases the glucose concentrations.

The body weight graph in fig. 1c illustrates the changes in mean body weight of six experimental groups over 45 days. Group 1 showed the most significant weight gain, consistently maintaining a higher body weight than the other group. Diabetic group (2) displayed substantial weight gain while the remaining treatment groups (3,4,5 and 6) demonstrated similar weight gain patterns. Notably, the synergistic group (6) maintained a relatively stable body weight than other groups.

Lipid parameter: Lipid parameters were assessed to evaluate changes in lipid metabolism. Figure 2 depicts serum levels of triglycerides (TG), total cholesterol (TC), high-density lipoprotein cholesterol (HDL-C), low-density lipoprotein cholesterol (LDL-C) and very low-density lipoprotein cholesterol (VLDL-C). All groups showed statistically significant differences ($P < 0.0001$) compared to the normal control.

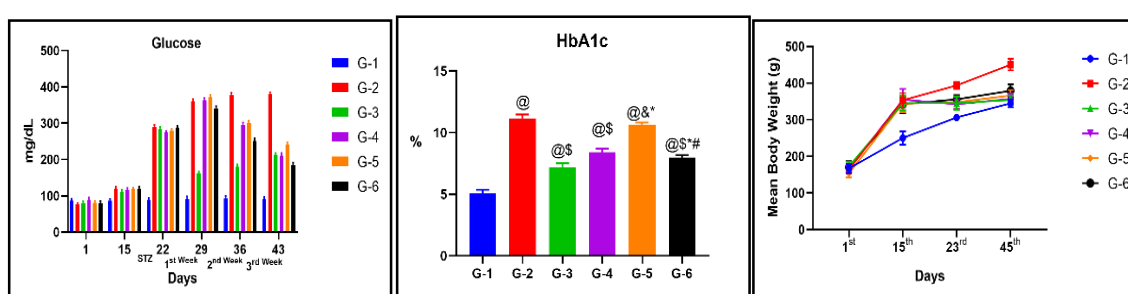


Fig. 1a

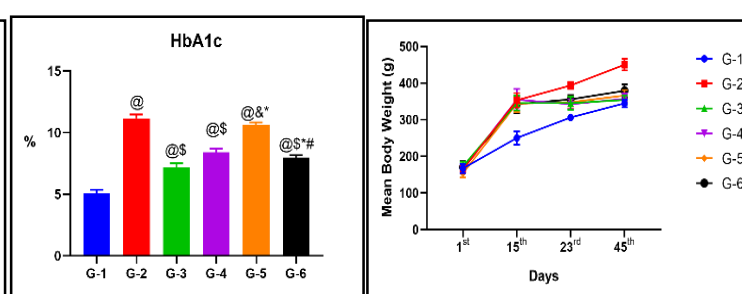


Fig. 1b

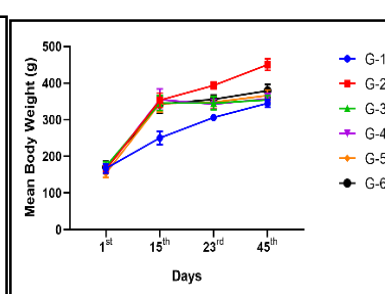


Fig. 1c

Fig. 1a, b and c; Effect of *C. cuspidatus* leaf extract, para-coumaric acid, metformin and synergistic effect streptozotocin on oral glucose tolerance test, glycated hemoglobin and body weight. In this experiment, all error bars represent the mean \pm SEM. Here, @ represents G1 vs G2; G3; G4; G5; and G6. \$ represent G2 vs G3; G4; G5; and G6. & represent G3 vs G4; G5 and G6. * Represent G4 vs G5; and G6. # Represent G5 vs G6. @\\$&#* p<0.05 implying statistically significant in glucose and HbA1c. The data were analyzed using one-way ANOVA followed by the Tukey test. Note: G1- Normal; G2 – Diabetic Control; G3 – Metformin; G4 – *C. cuspidatus*; G5 – para-Coumaric acid; and G6 – *C. cuspidatus* + para-Coumaric acid

The diabetic group (2) exhibited elevated TC, TG, VLDL and LDL levels, along with reduced HDL-C levels, indicative of diabetic dyslipidemia. Treatment with *para*-coumaric acid and the synergistic combination resulted in comparable improvements. Metformin and *C. cuspidatus* showed limited effects on VLDL-C and HDL-C. The synergistic group demonstrated a substantial reduction in TC, TG, LDL-C and VLDL-C, coupled with a significant increase in HDL-C, resembling the normal control. These findings suggest that *para*-coumaric acid possesses antilipidemic properties and that the synergistic combination effectively manages diabetic dyslipidemia.

Renal markers: Fig. 3 demonstrates the effects of *C. cuspidatus*, *para*-coumaric acid, metformin and synergistic

combination on serum renal indicators, namely blood urea nitrogen (BUN), creatinine and uric acid. All treatment groups exhibited statistically significant reductions ($P < 0.0001$) compared to the normal control. The diabetic control group displayed significantly elevated BUN, creatinine and uric acid levels, indicative of impaired renal function and proteinuria. While both *C. cuspidatus* and *p*-coumaric acid combination significantly reduced renal markers, the synergistic group demonstrated the most pronounced effects on BUN, creatinine and uric acid levels. Groups 5 and 3 exhibited similar, moderated reductions in renal markers. These findings suggest that synergistic therapy effectively addresses diabetic microvascular complications.

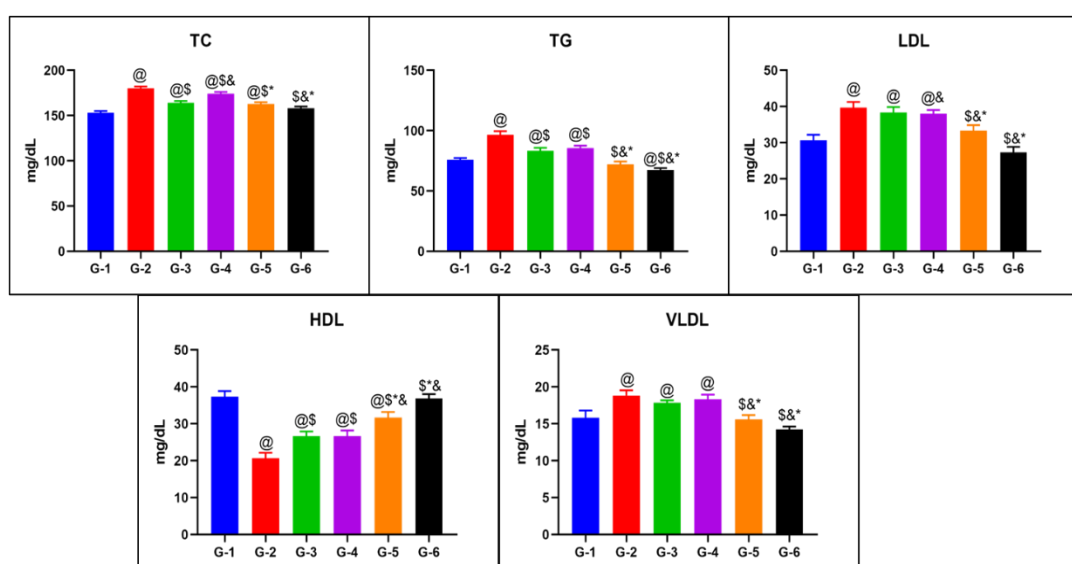


Fig. 2: Effect of *C. cuspidatus* leaf extract, *para*-coumaric acid, metformin and synergistic effect streptozotocin on lipid parameters. In this experiment, all error bars represent the mean \pm SEM. Here, @ represents G1 vs G2; G3; G4; G5; and G6. \$ represent G2 vs G3; G4; G5; and G6. & represent G3 vs G4; G5 and G6. * Represent G4 vs G5; and G6. # Represent G5 vs G6. @\$&*# $P < 0.0001$ implying statistically significant in all lipid parameters. The data were analyzed using one-way ANOVA followed by the Tukey test. Note: G1- Normal; G2 – Diabetic Control; G3 – Metformin; G4 – *C. cuspidatus*; G5 – *para*-Coumaric acid; and G6 – *C. cuspidatus* + *para*-Coumaric acid

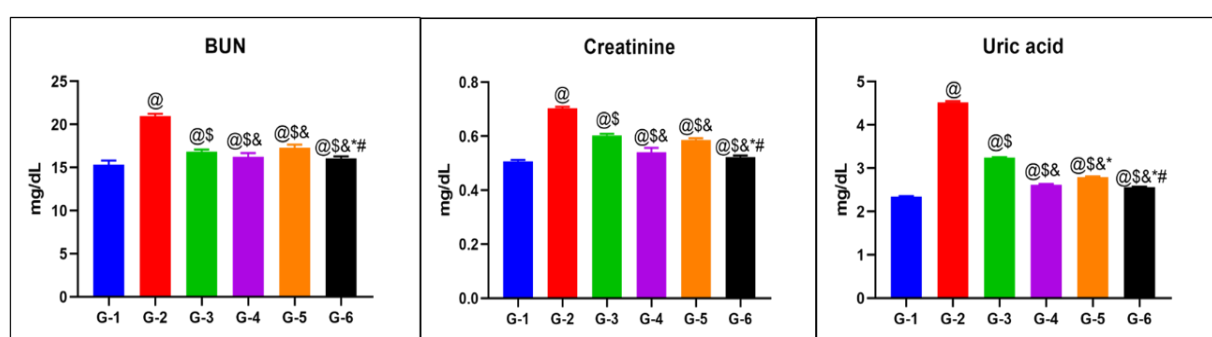


Fig. 3: Effect of *C. cuspidatus* leaf extract, *para*-coumaric acid, metformin and synergistic effect streptozotocin on lipid parameters. In this experiment, all error bars represent the mean \pm SEM. Here, @ represents G1 vs G2; G3; G4; G5; and G6. \$ represent G2 vs G3; G4; G5; and G6. & represent G3 vs G4; G5 and G6. * Represent G4 vs G5; and G6. # Represent G5 vs G6. @\$&*# $P < 0.0001$ implying statistically significant in all renal markers. The data were analyzed using one-way ANOVA followed by the Tukey test. Note: G1- Normal; G2 – Diabetic Control; G3 – Metformin; G4 – *C. cuspidatus*; G5 – *para*-Coumaric acid; and G6 – *C. cuspidatus* + *para*-Coumaric acid

Antioxidant and Oxidative indicators in the kidney: Fig. 4a illustrates the effects of *C. cuspidatus*, *para*-coumaric acid, metformin and synergistic combination on tissue antioxidant defense markers in the kidney. All enzymatic (SOD, CAT, GPx) and non-enzymatic (GSH) antioxidants demonstrated statistically significant differences ($P < 0.0001$) compared to the normal control. The control group exhibited the highest antioxidant levels followed by 6, 5, 4 and 3. In contrast, the diabetic control group displayed lower antioxidant levels, suggesting overwhelmed antioxidant enzymes and elevated oxidative stress.

Fig. 4b demonstrates the impact of *C. cuspidatus*, *para*-coumaric acid, metformin and synergistic combination intervention on tissue oxidant stress levels in the kidney. The control group displayed average levels of primary (ROS), lipid peroxide product of MDA and secondary (nitric oxide) oxidant stress markers. The diabetic group exhibited elevated oxidative and lipid peroxidation markers (MDA), indicative of endothelial damage. The synergistic group, followed by *C. cuspidatus*, metformin and *para*-coumaric acid, demonstrated protective effects, reducing oxidative stress markers and enhancing antioxidant enzyme activity.

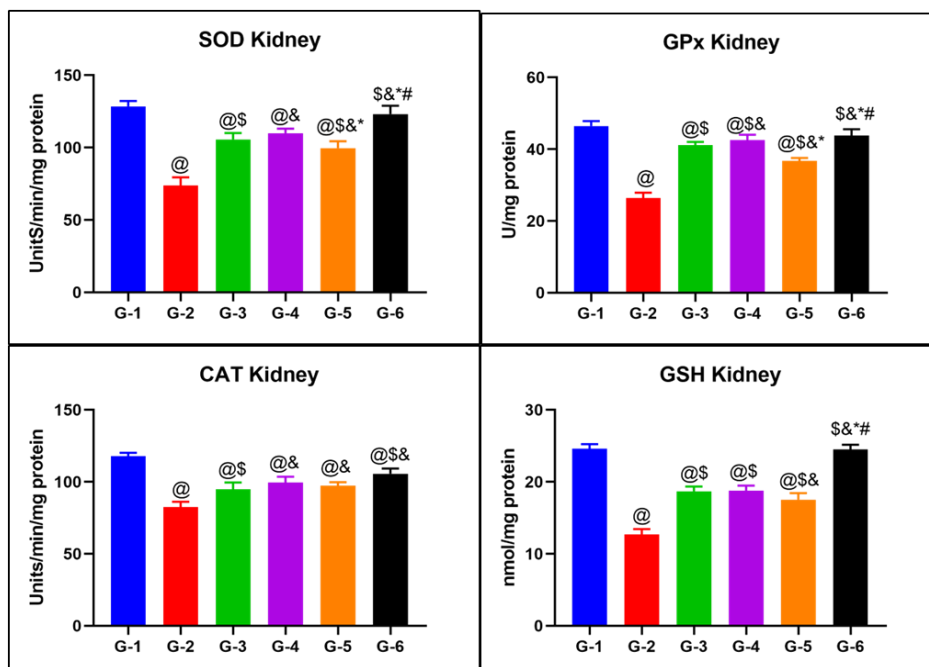


Fig. 4a: Effect of *C. cuspidatus* leaf extract, *para*-coumaric acid, metformin and synergistic effect streptozotocin on enzymatic and non-enzymatic antioxidant parameters. In this experiment, all error bars represent the mean \pm SEM. Here, @ represents G1 vs G2; G3; G4; G5; and G6. \\$ represent G2 vs G3; G4; G5; and G6. & represent G3 vs G4; G5 and G6. * Represent G4 vs G5; and G6. # Represent G5 vs G6. @\\$&*# $P < 0.0001$ implying statistically significant in all antioxidant assays. The data were analyzed using one-way ANOVA followed by the Tukey test. Note: G1- Normal; G2 – Diabetic Control; G3 – Metformin; G4 – *C. cuspidatus*; G5 – *para*-Coumaric acid; and G6 – *C. cuspidatus* + *para*-Coumaric acid

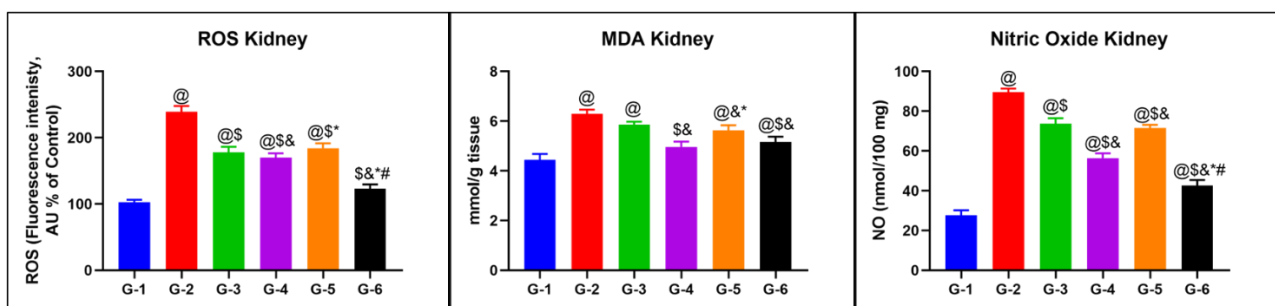


Fig. 4b: Effect of *C. cuspidatus* leaf extract, *para*-coumaric acid, metformin and synergistic effect streptozotocin on oxidative stress indicators. In this experiment, all error bars represent the mean \pm SEM. Here, @ represents G1 vs G2; G3; G4; G5; and G6. \\$ represent G2 vs G3; G4; G5; and G6. & represent G3 vs G4; G5 and G6. * Represent G4 vs G5; and G6. # Represent G5 vs G6. @\\$&*# $P < 0.0001$ implying statistically significant in all oxidant stress markers. The data were analyzed using one-way ANOVA followed by the Tukey test. Note: G1- Normal; G2 – Diabetic Control; G3 – Metformin; G4 – *C. cuspidatus*; G5 – *para*-Coumaric acid; and G6 – *C. cuspidatus* + *para*-Coumaric acid

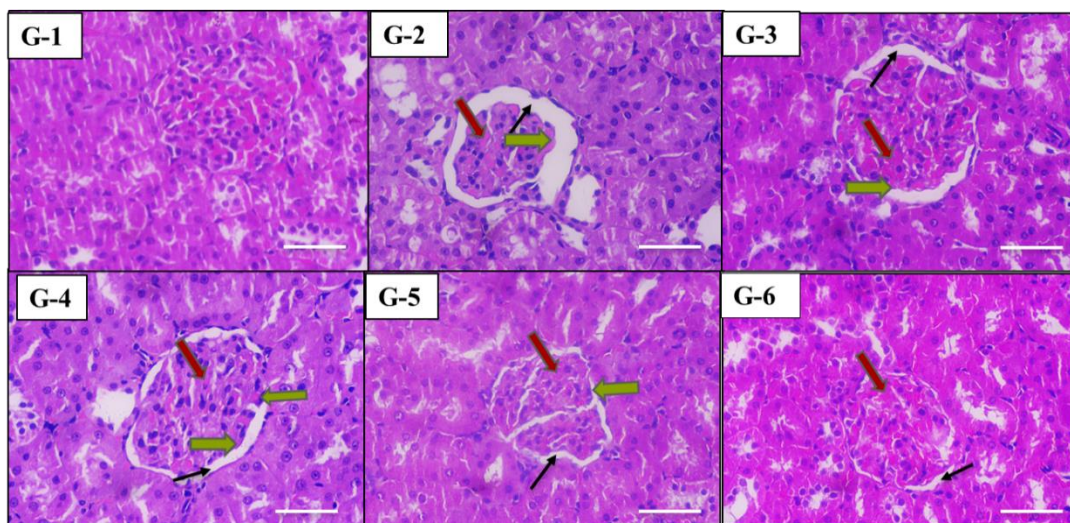


Fig. 5: Effect of *Chamaecostus cuspidatus* and *para*-coumaric acid on diabetic rats' kidney at 45th day.

The H&E-stained rat renal corpuscle is depicted in a microscopic image. The red lines represent mesangial diffusion and nodules; the green arrow indicates the capsular space between the visceral and parietal layer; the dark brown arrow indicates local thickening of the basement membrane; and the black arrows indicate the thickening of the glomerular basement membrane (GBM). Scale bar: 50 μ m

Histopathological of Renal tissue: Fig. 5 illustrates the histological changes in renal corpuscle tissue. The normal control group exhibited a normal structure and arrangement of the renal corpuscle, tubular structure and Bowman's capsule. In contrast, the diabetic group displayed severe-to-chronic damage, including mesangial lesion, tuber-sclerosis and glomerular-based membrane thickening, indicative of a compromised filtration barrier and increased proteinuria associated with diabetic glomerulosclerosis. The metformin group showed mild-to-moderate thickening of the glomerular basement membrane and minor mesangial changes. *C. cuspidatus* resulted in partial restoration of the Bowman's capsule structure with local thickening of the basement membrane and mild-to-moderate mesangial enlargement and inflammation.

The *para*-coumaric acid group exhibited improved mesangial expansion, moderate GBM thickening and a partially restored Bowman's capsule with minor disassociation of junction between tubular. The synergistic combination demonstrated significant recovery of the Bowman's capsule structure, with slight congestion of glomerular tufts resembling the early-diabetic nephropathy. These histology findings suggest that the synergistic effect restored the specialized extracellular matrix of the glomerular basement membrane, leading to improved filtration function.

Conclusion

The present study demonstrated that a synergistic combination of *C. cuspidatus* leaf extract (100mg/kg) and *para*-coumaric acid (20mg/kg) was more effective than metformin in mitigating renal damage induced by streptozotocin-induced diabetes in Wistar rats. *C. cuspidatus* exhibited promising effects in reducing glucose and renal markers, while *para*-coumaric acid demonstrated a reducing

effect on lipoproteins. This combination therapy exhibited beneficial effects on hematological parameters, renal function markers, antioxidant status and oxidative stress indicators, suggesting its potential as a promising approach for the prevention and management of diabetic nephropathy.

Given the promising lipid-regulating effects of *para*-coumaric acid, future research on combining it with metformin could be an attractive avenue for addressing diabetic nephropathy, potentially offering an alternative to stand-alone therapy with either compound or commercial synthetic medications.

Acknowledgement

The authors are grateful to the Vellore Institute of Technology for providing lab facilities to complete research work.

References

1. Albasher G., Alwahaibi M., Abdel-Daim M.M., Alkahtani S. and Almeer R., Protective effects of *Artemisia judaica* extract compared to metformin against hepatorenal injury in high-fat diet/streptozotocin-induced diabetic rats, *Environ. Sci. Pollut. Res.*, **27**, 40525–40536 (2020)
2. Amalan V., Vijayakumar N., Indumathi D. and Ramakrishnan A., Antidiabetic and antihyperlipidemic activity of *p*-coumaric acid in diabetic rats, the role of pancreatic GLUT 2: *In-vivo* approach, *Biomed. Pharmacother.*, **84**, 230–236 (2016)
3. Bayne K., Revised Guide for the Care and Use of Laboratory Animals available, American Physiological Society, The Physiologist (1996)
4. Chakrabarti R., Diabetes and Atherosclerosis, *Br. Med. J.*, **1**, 1170 (1966)
5. Cullinan S.B. and Diehl J.A., Coordination of ER and oxidative

stress signaling: The PERK/Nrf2 signaling pathway, *Int. J. Biochem. Cell Biol.*, **38**, 317–332 (2006)

6. Diabetes Federation International, IDF Diabetes Atlas, International Diabetes Federation (2019)

7. Förstermann U., Oxidative stress in vascular disease: causes, defense mechanisms and potential therapies, *Nat. Clin. Pract. Cardiovasc. Med.*, **5**, 338–349 (2008)

8. Hajam Y.A., Kumar R., Reshi M.S., Rawat D.S., AlAsmari A.F., Ali N., Ali Y.S.M. and Ishtikhar M., Administration of Costus igneus Nak leaf extract improves diabetic-induced impairment in hepatorenal functions in male albino rats, *J. King Saud Univ. - Sci.*, **34**, 101911 (2022)

9. Kalailingam P., Balasubramanian K., Kannaiyan B., Mohammed A.K.N., Meenakshisundram K., Tamilmani E. and Kaliaperumal R., Isolation and quantification of flavonoids from ethanol extract of Costus igneus rhizome (CiREE) and impact of CiREE on hypoglycaemic, electron microscopic studies of pancreas in streptozotocin (STZ)-induced diabetic rats, *Biomed. Prev. Nutr.*, **3**, 285–297 (2013)

10. Kalailingam P., Kannaiyan B., Tamilmani E. and Kaliaperumal R., Efficacy of natural diosgenin on cardiovascular risk, insulin secretion and beta cells in streptozotocin (STZ)-induced diabetic rats, *Phytomedicine*, **21**, 1154–1161 (2014)

11. Krishnan K., Mathew L.E., Vijayalakshmi N.R. and Helen A., Anti-inflammatory potential of β -amyrin, a triterpenoid isolated from Costus igneus, *Inflammopharmacology*, **22**, 373–385 (2014)

12. Lu Q., Zheng R., Zhu P., Bian J., Liu Z. and Du J., Hinokinin alleviates high-fat diet/streptozotocin-induced cardiac injury in mice through modulation in oxidative stress, inflammation and apoptosis, *Biomed. Pharmacother.*, **137**, 111361 (2021)

13. Marklund S. and Marklund G., Involvement of the Superoxide Anion Radical in the Autoxidation of Pyrogallol and a Convenient Assay for Superoxide Dismutase, *Eur. J. Biochem.*, **47**, 469–474 (1974)

14. Moron S.M., Depierre W.J. and Mannervik B., Levels of glutathione-S-transferase activities in rat lung and liver, *Biochim. Biophys. Acta*, **582**, 67–78 (1979)

15. Pedrol N., Handbook of Plant Ecophysiology Techniques, Handb. Plant Ecophysiol. Tech (2001)

16. PonnaniKajamideen M., Rajeshkumar S., Vanaja M. and Annadurai G., *In-vivo* Type 2 Diabetes and Wound-Healing Effects of Antioxidant Gold Nanoparticles Synthesized Using the Insulin Plant Chamaecostus cuspidatus in Albino Rats, *Can. J. Diabetes*, **43**, 82-89.e6 (2019)

17. Rotruck J.T., Pope A.L., Ganther H.E., Swanson A.B., Hafeman D.G. and Hoekstra W.G., Selenium: Biochemical role as a component of glutathione peroxidase, *Science*, **179**, 588–590 (1973)

18. Sinha A.K., Colorimetric assay of catalase, *Anal. Biochem.*, **47**, 389–394 (1972)

19. Song L., Zhang J., Lai R., Li Q., Ju J. and Xu H., Chinese Herbal Medicines and Active Metabolites: Potential Antioxidant Treatments for Atherosclerosis, *Front. Pharmacol.*, **12**, 1–20 (2021)

20. Vargas-Vargas M.A., Saavedra-Molina A., Gómez-Barroso M., Peña-Montes D., Cortés-Rojo C., Miguel H., Trujillo X. and Montoya-Pérez R., Dietary Iron Restriction Improves Muscle Function, Dyslipidemia and Decreased Muscle Oxidative Stress in Streptozotocin-Induced Diabetic Rats, *Antioxidants*, **11**, 731 (2022)

21. Webber S., International Diabetes Federation, Diabetes Research and Clinical Practice (2013)

22. Wickramasinghe A.S.D., Attanayake A.P. and Kalansuriya P., Biochemical characterization of high-fat diet-fed and low dose streptozotocin-induced diabetic Wistar rat model, *J. Pharmacol. Toxicol. Methods*, **113**, 107144 (2022)

23. Wu T., Ding L., Andoh V., Zhang J. and Chen L., The Mechanism of Hyperglycemia-Induced Renal Cell Injury in Diabetic Nephropathy Disease: An Update, *Life*, **13**, 1–18 (2023).

(Received 08th November 2024, accepted 09th January 2025)